

# Temperature dependence of the tensile properties of single-walled carbon nanotubes: $O(N)$ tight-binding molecular-dynamics simulations

Gülay Dereli\* and Banu Süngü

*Department of Physics, Yıldız Technical University, 34210 Istanbul, Turkey*

(Received 17 September 2006; revised manuscript received 24 January 2007; published 14 May 2007)

This paper examines the effect of temperature on the structural stability and mechanical properties of 20-layered (10,10) single-walled carbon nanotubes (SWCNTs) under tensile loading using an  $O(N)$  tight-binding molecular-dynamics simulation method. We observed that (10,10) tube can sustain its structural stability for the strain values of 0.23 in elongation and 0.06 in compression at 300 K. Bond-breaking strain value decreases with increasing temperature under stretching but not under compression. The elastic limit, Young's modulus, tensile strength, and Poisson ratio are calculated as 0.10, 0.395 TPa, 83.23 GPa, and 0.285, respectively, at 300 K. In the temperature range from 300 to 900 K, Young's modulus and the tensile strengths decrease with increasing temperature while the Poisson ratio increases. At higher temperatures, Young's modulus starts to increase while the Poisson ratio and tensile strength decrease. In the temperature range from 1200 to 1800 K, the SWCNT is already deformed and softened. Applying strain on these deformed and softened SWCNTs does not follow the same pattern as in the temperature range of 300 to 900 K.

DOI: [10.1103/PhysRevB.75.184104](https://doi.org/10.1103/PhysRevB.75.184104)

PACS number(s): 61.46.Fg, 62.25.+g, 62.20.Dc, 62.20.Fe

## I. INTRODUCTION

Tensile properties of single-walled carbon nanotubes (SWCNTs) have been widely investigated by experimental and theoretical techniques. Experimentally, Young's modulus of SWCNTs is measured ranging from 0.9 to 1.9 TPa in Ref. 1. In the scanning electron microscopy measurements of Ref. 2 SWCNT ropes broke at the strain values of 5.3% or lower and the determined mean values of breaking strength and Young's modulus are 30 and 1002 GPa, respectively. Atomic force microscopy and scanning gate microscopy measurements<sup>3</sup> show that SWCNTs can sustain elongations as great as 30% without breaking.

On the other hand, the *ab initio* simulation study of SWCNTs (Ref. 4) showed that Young's modulus and Poisson ratio values of the tubes range from 0.5 to 1.1 TPa and from 0.11 to 0.19, respectively. The Young modulus and Poisson ratio of armchair nanotubes are given as 0.764 TPa and 0.32, respectively, in Ref. 5. Young's moduli, of (10,0), and (8,4), and (10,10) tubes are calculated as 1.47, 1.10, and 0.726 TPa, respectively, in Ref. 6. The results of Ref. 7 proposed that the structural failure should occur at 16% for zigzag and above 24% for armchair tubes. An empirical force-constant model of Ref. 8 gave Young's modulus between 0.971 and 0.975 TPa and Poisson ratio between 0.277 and 0.280. An empirical pair potential simulation of Ref. 9 gave Young's modulus between 1.11 and 1.258 TPa and the Poisson ratio between 0.132 and 0.151. Continuum shell model of Ref. 10 calculated the elastic modulus as 0.94 TPa and the maximum stress and failure strain values as 70 and 88 GPa, and 11%, and 15% for (17,0) and (10,10) tubes, respectively. Finite-element method<sup>11</sup> determined the strength of CNTs between 77 and 101 GPa and Poisson ratio between 0.31 and 0.35. Analytical model in Ref. 12 found the tensile strength as 126.2 GPa of armchair tubes to be stronger than that (94.56 GPa) of zigzag tubes and the failure strains are 23.1% for armchair and 15.6%–17.5% for zigzag tubes. Molecular-dynamics (MD) simulations of Refs. 13–17 determined

Young's modulus between 0.311 and 1.017 TPa for SWCNT. We found Young's modulus, tensile strength, and the Poisson ratio as 0.311 TPa, 4.92 GPa, and 0.287 for (10,10) tubes in Ref. 16. Goze *et al.*<sup>18</sup> calculated Young's modulus as 0.423 TPa and Poisson ratio as 0.256 for (10,10) tube. Non-linear elastic properties of SWCNTs under axial tension and compression were studied by Xiao and co-workers<sup>19,20</sup> using MD simulations with the second-generation Brenner potential. They showed that the energy change of the nanotubes is a cubic function of the tensile strains, both in tension and under compression. The maximum elongation strains are 15% and 17% for zigzag and armchair tubes, respectively. Also, the maximum compression strain decreases with increasing tube diameter, and it is almost 4% for (10,10) tube. Sammalkorpi *et al.*<sup>21</sup> studied the effects of vacancy-related defects on the mechanical characteristics of SWCNTs by employing MD simulations and continuum theory. They calculated Young's modulus for perfect SWCNTs as 0.7 TPa. They showed that at 10 K temperature, the critical strains of (5,5) and (10,10) tubes are 26% and 27%, respectively; also, tensile strength is 120 GPa. On the other hand, for (9,9) and (17,0) tubes, the critical strains are found as 22% and 21%, respectively, and tensile strength is 110 GPa. Wang *et al.*<sup>22</sup> investigated the compression deformation of SWCNTs by MD simulations using the Tersoff-Brenner potential to describe the interactions of carbon atoms. They determined that for the SWCNTs whose diameters range from 0.5 to 1.7 nm and lengths range from 7 to 19 nm, Young's modulus ranges from 1.25 to 1.48 TPa. Yeak *et al.*<sup>23</sup> used MD and tight-binding molecular-dynamics (TBMD) methods to examine the mechanical properties of SWCNTs under axial tension and compression. Their results showed that Young's modulus of the tubes is around 0.53 TPa; the maximum strain under axial tension is 20% for (12,12) and (7,7) tubes, and also under this strain rate, the tensile stresses are 100 and 90 GPa, respectively. Many elastic characteristics such as Young's modulus show a wide variation (0.3–1.48 TPa) in all reported results in literature. These results are obtained at room

temperature or without the mention of the temperature. The following reasons may be given for variety of results: (i) Young's modulus depends on the tube diameter and the chirality, (ii) different values are used for the wall thickness, (iii) different procedures are applied to represent the strain, and (iv) accuracy of the applied methods (first-principles methods in comparison with empirical model potentials).

SWCNTs will be locally subjected to abrupt temperature increases in electronic circuits and the temperature increase affects their structural stability and the mechanical properties. MD simulation studies on the mechanical properties of the SWCNTs at various temperatures under tensile loading simulations can be found in Refs. 24–28. Nardelli *et al.*<sup>24</sup> showed that all tubes are brittle at high strains and low temperatures, while at low strains and high temperatures armchair nanotubes can be completely or partially ductile. In zigzag tubes, ductile behavior is expected for tubes with  $n < 14$  while larger tubes are completely brittle. Raravikar *et al.*<sup>25</sup> showed that between 0 and 800 K temperature range, radial Young's modulus of nanotubes decreases with increasing temperature and its slope is  $-7.5 \times 10^{-5}$  (1/K). Wei *et al.*<sup>26,27</sup> studied the tensile yielding of SWCNTs and multi-walled carbon nanotubes under continuous stretching using MD simulations and a transition-state theory based model. They showed that the yield strain decreases at higher temperatures and at slower strain rates. The tensile yield strain of SWCNT has a linear dependence on the temperature and has a logarithmic dependence on the strain rate. The slope of the linear dependence increases with temperature. From their results, it is shown that the yield strain of (10,0) tube decreased from 18% to 5% for the temperature range increasing from 300 to 2400 K and for the different strain rates. Another MD simulation study performed by Jeng *et al.*<sup>28</sup> investigated the effect of temperature and vacancy defects on tensile deformation of (10,0), (8,3), and (6,6) tubes of similar radii. Their Young's modulus and Poisson ratio values range from 0.92 to 1.03 TPa and 0.36–0.32, respectively. Their simulations also demonstrate that the values of the majority of the considered mechanical properties decrease with increasing temperature and increasing vacancy percentage.

In this study, the effect of temperature increase on the structural stability and mechanical properties of (10,10) armchair SWCNT under tensile loading is investigated by using  $O(N)$  TBMD simulations. Extensive literature survey is given in order to show the importance of our present study. The armchair 20-layered (10,10) SWCNT is chosen in the present work because it is one of the most synthesized nanotube in the experiments. We questioned how the strain energy of these nanotubes changes for positive and negative strain values at high temperatures. Along with the high-temperature stress-strain curves, we displayed the bond-breaking strain values through total-energy graphs. Mechanical properties (Young's modulus, Poisson ratio, tensile strength, and elastic limit) of this nanotube are reported at high temperatures.

## II. METHOD

Traditional TB theory solves the Schrödinger equation by direct matrix diagonalization, which results in cubic scaling

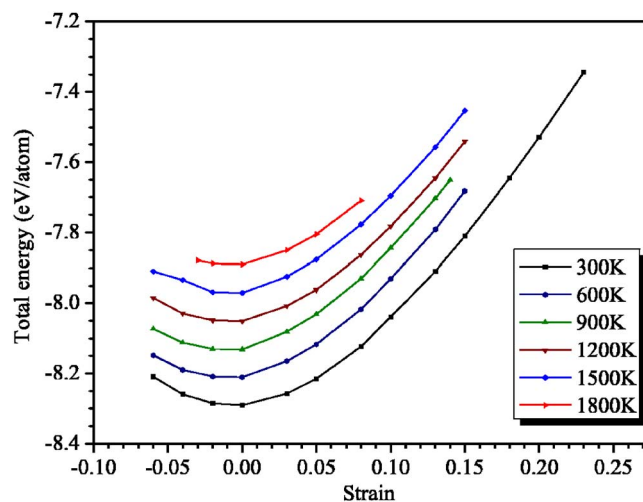


FIG. 1. (Color online) Total energy per atom curves as a function of strain at different temperatures (negative strain values correspond to compression).

with respect to the number of atoms  $O(N^3)$ . The  $O(N)$  methods, on the other hand, make the approximation that only the local environment contributes to the bonding and hence the bond energy of each atom. In this case, the run time would be in linear scaling with respect to the number of atoms. Dereli and co-workers<sup>29,30</sup> have improved and successfully applied the  $O(N)$  TBMD technique to SWCNTs. In this work, using the same technique, we performed SWCNT simulations depending on conditions of temperature and uniaxial strain. The electronic structure of the simulated system is calculated by a TB Hamiltonian so that the quantum-mechanical many-body nature of the interatomic forces is taken into account. Within a semiempirical TB, the matrix elements of the Hamiltonian are evaluated by fitting a suitable database. TB hopping integrals, repulsive potential, and scaling law are fixed in the program.<sup>31,32</sup> Application of the technique to SWCNTs can be seen in our previous studies.<sup>16,29,30</sup>

An armchair (10,10) SWCNT consisting of 400 atoms with 20 layers is simulated. Periodic boundary condition is applied along the tube axis. Velocity Verlet algorithm along with the canonical ensemble molecular dynamics (NVT) is used. Our simulation procedure is as follows: (i) The tube is simulated at a specified temperature for a 3000 MD steps of run with a time step of 1 fs. This eliminates the possibility of the system to be trapped in a metastable state. We wait for the total energy per atom to reach the equilibrium state. (ii) Next, uniaxial strain is applied to the tubes. We further simulated the deformed tube structure (the under uniaxial strain) for another 2000 MD steps. In our study, while the nanotube is axially elongated or contracted, reduction or enlargement of the radial dimension is observed. Strain is obtained from  $\varepsilon = (L - L_0)/L_0$ , where  $L_0$  and  $L$  are the tube lengths before and after the strain, respectively. We applied the elongation and compression and calculated the average total energy per atom. Following this procedure, we examined the structural stability, total energy per atom, stress-strain curves, elastic limit, Young's modulus, tensile strength, and Poisson ratio of

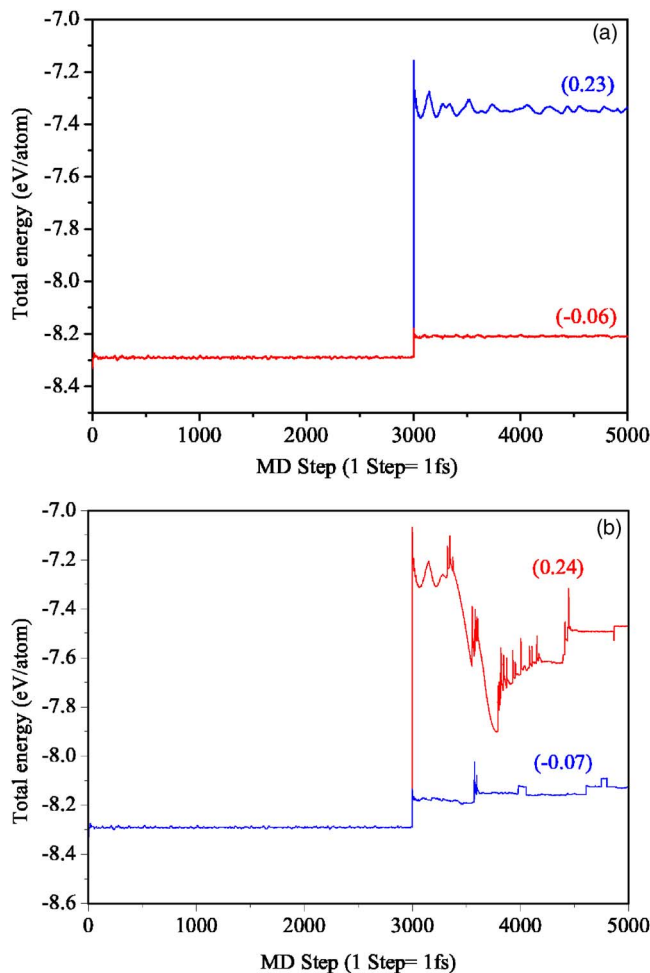


FIG. 2. (Color online) (a) (10,10) SWCNT is stable for the strains of 0.23 and  $-0.06$  at 300 K. (b)(Color online) Bond breakings are observed between the carbon atoms for the strains of 0.24 and  $-0.07$  at 300 K. System is not in equilibrium.

the (10,10) tube as a function of temperature.

The stress is determined from the resulting force acting on the tube per cross-sectional area under stretching. The cross-sectional area  $S$  of the tube is defined by  $S=2\pi R\delta R$ , where  $R$  and  $\delta R$  are the radius and the wall thickness of the tube, respectively. We have used  $3.4\text{ \AA}$  for wall thickness. Mechanical properties are calculated from the stress-strain curves. Elastic limit is obtained from the linear regions of the stress-strain curves. Young's modulus, which shows the resistivity of a material to a change in its length, is determined from the slope of the stress-strain curve at studied temperatures. The tensile strength can be defined as the maximum stress which may be applied to the tube without perturbing its stability. Poisson ratio, which is a measure of the radial reduction or expansion of a material under tensile loading, can be defined as

$$\nu = -\frac{1}{\varepsilon} \left( \frac{R - R_0}{R_0} \right),$$

where  $R$  and  $R_0$  are the tube radius at the strain  $\varepsilon$  and before the strain, respectively.

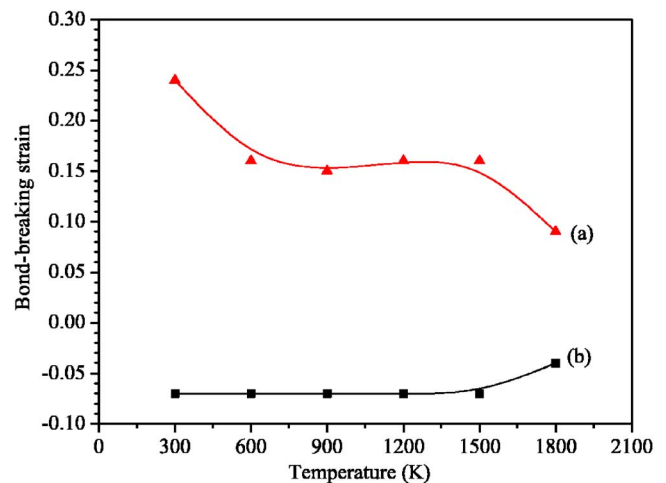


FIG. 3. (Color online) Bond-breaking strain variations as a function of temperature for (a) tension, and (b) compression.

### III. RESULTS AND DISCUSSION

In Fig. 1, we present the total energy per atom of the (10,10) SWCNT as a function of strain. Several strain values are applied. The positive values of strain correspond to elongation and the negative values to compression. We obtained the total energy per atom vs strain curves in the temperature range between 300 and 1800 K in steps of 300 K. Total energy per atom increases as we increase the temperature. An asymmetric pattern is observed in these curves. Repulsive forces are dominant in the case of compression. SWCNT does not have a high strength for compression as much as for elongation. (10,10) SWCNT is stable up to 0.06 strain in compression in the temperature range between 300 and 1500 K and 0.03 at 1800 K. In elongation, (10,10) SWCNT is stable up to 0.23 strain at 300 K. As we increase the temperature, the tube is stable up to 0.15 in elongation until 1800 K. At 1800 K, we can only apply the strain of 0.08 in elongation before bond breakings. Figure 2(a) shows the variation of the total energy per atom during simulations for the strain values of 0.23 in elongation and 0.06 in compression at 300 K. This figure indicates that the tube can sustain its structural stability up to these strain values. Beyond these, bond breakings between the carbon atoms are observed at the strain values of 0.24 in elongation and 0.07 in compression, as given in Fig. 2(b). In Fig. 2(b), sharp peaks represent the disintegrations of atoms from the tube. Next, bond-breaking strains are studied with increasing temperature. In Fig. 3, we show the bond-breaking strain values with respect to temperature: as the temperature increases, disintegration of atoms from their places is possible at lower strain values due to the thermal motion of atoms. But this is not the case for compression, as can be seen in Fig. 3. Some examples of the variation of the total energy as a function of MD steps under uniaxial strain values at various temperatures are given in Figs. 4 and 5. Figs. 4(a) and 5(a) show that the tube can sustain its structural stability for strain values of 0.14 in elongation and 0.06 in compression at 900 K, and 0.08 in elongation and 0.03 in compression at 1800 K, respectively. Beyond these points, bond breakings between carbon atoms are

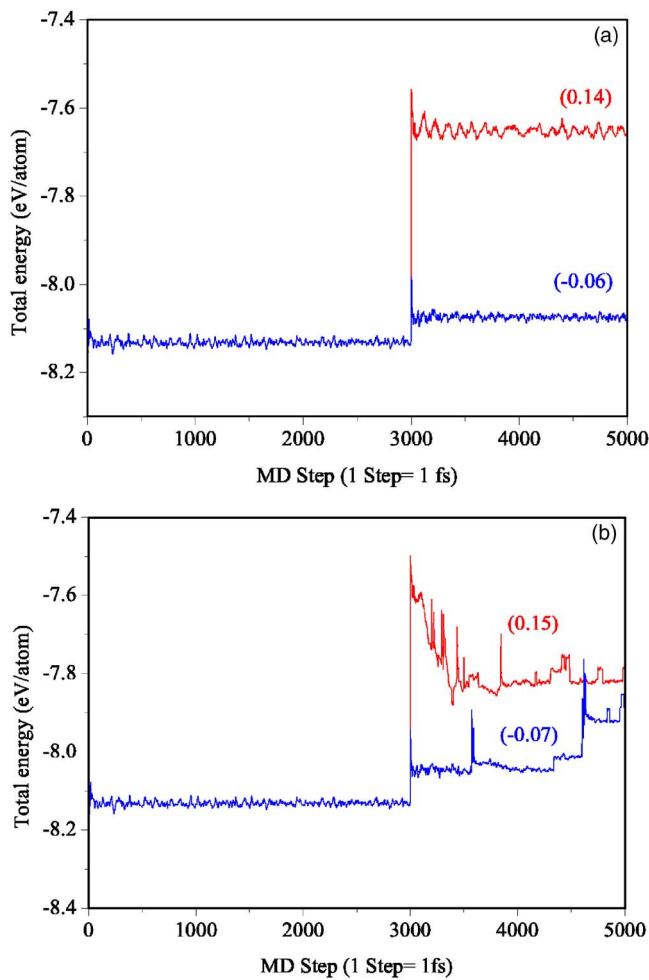


FIG. 4. (Color online) (a) (10,10) SWCNT is stable for the strains of 0.14 and  $-0.06$  at 900 K. (b) Bond breakings are observed between the carbon atoms for the strains of 0.15 and  $-0.07$  at 900 K. System is not in equilibrium.

observed at the strain values of 0.15 in elongation and 0.07 in compression at 900 K [Fig. 4(b)], and 0.09 in elongation and 0.04 in compression at 1800 K [Fig. 5(b)].

The stress-strain curves of the tube are given in Fig. 6 at studied temperatures. Our results show that the temperature has a significant influence on the stress-strain behavior of the tubes. The stress-strain curves are in the order of increasing temperatures between 300 and 900 K. Stress value increases with increasing temperature. On the other hand, between 1200 and 1800 K, the stress value decreases with increasing temperature. This is due to the smaller energy difference under tensile loading with respect to 300–900 K temperature range. This result can also be followed in the total-energy changes observed in Figs. 2(b), 4(b), and 5(b).

Table I gives a summary of the variations of the mechanical properties of (10,10) SWCNT with temperature. As given in Table I, elastic limit has the same value (0.10) in the 300–900 K temperature range. It drops to 0.09 in the 1200–1500 K temperature range and to 0.08 at 1800 K. Young's modulus, Poisson ratio, and the tensile strength of the tube have been found to be sensitive to the temperature (Table I). Our calculated value at 300 K is 0.401 TPa. It

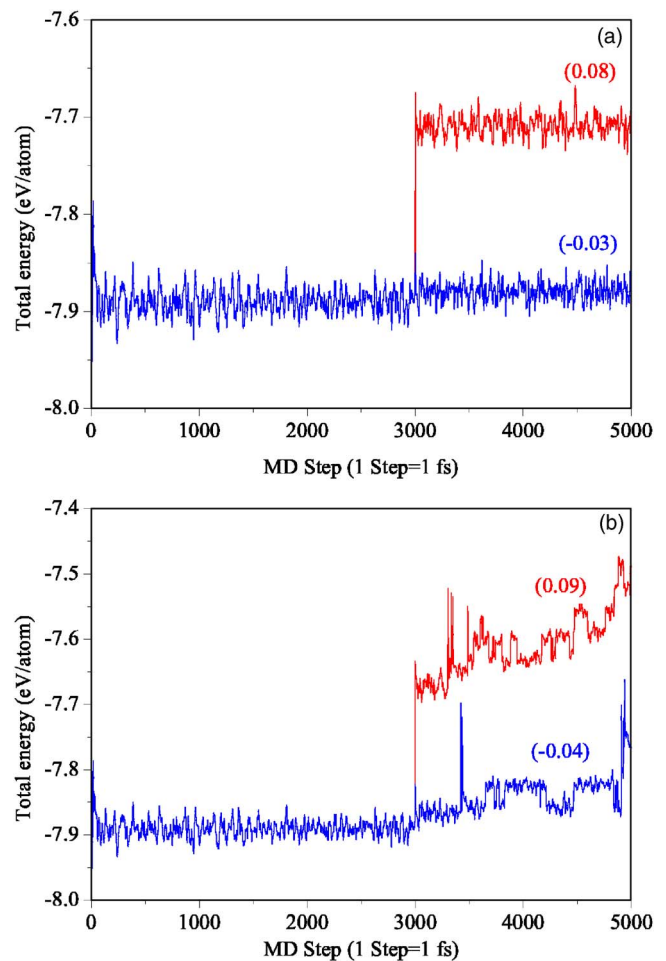


FIG. 5. (Color online) (a) (10,10) SWCNT is stable for the strains of 0.08 and  $-0.03$  at 1800 K. (b) Bond breakings are observed between the carbon atoms for the strains of 0.09 and  $-0.04$  at 1800 K. System is not in equilibrium.

decreases to 0.370 TPa at 600 K and to 0.352 TPa at 900 K. In this temperature range Young's modulus decreases by 12%. After 1200 K, as we increase the temperature to 1800 K, there is a 3% increase in Young's modulus. We determined the tensile strength of (10,10) tube as 83.23 GPa at 300 K. There is an abrupt decrease in tensile strength as we increase the temperature to 900 K. Between 900 and 1500 K temperature range, tensile strength does not change appreciably. At 1800 K, it drops to 43.78 GPa. We specified the Poisson ratio at 300 K as 0.3. Between 300 and 900 K temperature range, Poisson ratio increases to 0.339 (12.5%). This corresponds to the increase in the radial reduction. As we increase the temperature to 1200 K, its value drops to 0.315, and at 1800 K to 0.289. We can conclude that for 20-layered (10,10) SWCNT in the 300–900 K temperature range, Young's modulus and the tensile strengths decrease with increasing temperature while the Poisson ratio increases. At higher temperatures, Young's modulus and the tensile strengths start to increase while the Poisson ratio decreases. In the 1200–1800 K temperature range, the SWCNT is already deformed and softened. Applying strain on these deformed and softened SWCNT does not follow the same pattern in the 300–900 K temperature range.

TABLE I. High-temperature mechanical properties of (10,10) SWCNT.

Temperature (K)	Elastic limit	Young's modulus (TPa)	Tensile strength (GPa)	Poisson ratio
300	0.10	0.401	83.23	0.300
600	0.10	0.370	69.78	0.332
900	0.10	0.352	67.62	0.339
1200	0.09	0.360	67.33	0.315
1500	0.09	0.356	68.14	0.320
1800	0.08	0.365	43.78	0.289

#### IV. CONCLUSION

This paper reports the effect of temperature on the stress-strain curves, Young's modulus, tensile strength, Poisson ratio, and elastic limit of (10,10) SWCNT. Total energy per atom of the (10,10) tube increases with axial strain under elongation. We propose that SWCNTs do not have a high strength for compression as much as for elongation. This is due to the dominant behavior of repulsive forces in compression. At room temperature, the bond-breaking strain values of the tube are 0.24 in elongation and 0.07 in compression. We showed that as the temperature increases, the disintegration of atoms from their places is possible at lower strain values (0.09 at 1800 K) in elongation due to the thermal motion of atoms. But this is not the case for compression. For 20-layered SWCNT, bond-breaking negative strain values are temperature independent between 300 and 1500 K temperature range. Bond breakings occur at 0.07 compression in this temperature range. When we increase the number of layers to 50, bond-breaking negative strain value decreases from 0.07 to 0.05 and remains the same in this temperature range. However, this is not a robust property for negative strains. When we decrease, on the other hand, the layer size to 10, bond-breaking negative strain values vary with increasing temperature. We note that for short tubes the critical strain values for compressive deformations are dependent on the size of the employed supercell and therefore

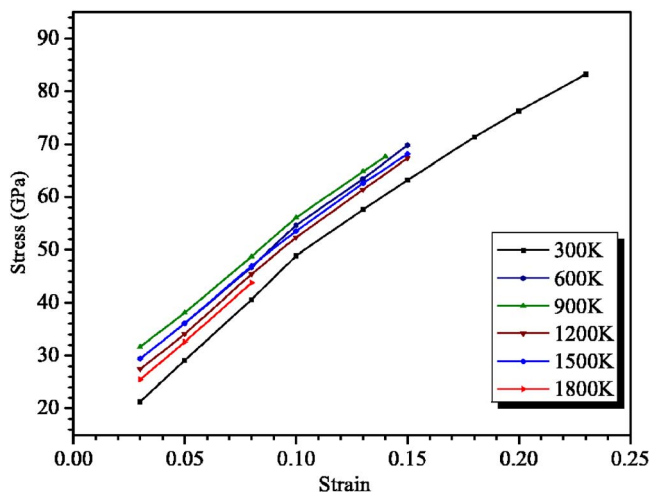


FIG. 6. (Color online) The stress-strain curves of (10,10) SWCNT at different temperatures.

they are an artifact of the calculation. In literature, various critical strain values were mentioned for the tube deformations. Our room-temperature critical strain values are in agreement with the experimental results of Ref. 3 and the computational results of Refs. 7, 10, and 12. MD simulations of Ref. 21 determined the critical strain value of (10,10) tube as 0.27 at 10 K. To our knowledge, the only reported temperature simulation study on tensile property comes from the MD simulation results of Ref. 26. They showed that the yield strain of (10,0) tube decreases from 0.18 to 0.05 for the temperature range increasing from 300 to 2400 K. Our results follow the same trend such that the bond-breaking strain values decrease with increasing temperature. In Ref. 20, the maximum compression strain of (10,10) tube is given as 0.04 using Brenner potential. Without the mention of temperature, we obtained this value at 1800 K.

We obtained the stress-strain curves in the temperature range between 300 and 1800 K. Our results show that the temperature has a significant influence on the stress-strain behavior of the tubes. (10,10) tube is brittle between 300 and 900 K and soft after 1200 K. The elastic limit decreased from 0.10 to 0.08 with increasing temperature. There is a wide range of values given in literature for Young's modulus of SWCNTs due to the accuracy of the method and the choice of the wall thickness of the tube. The experimental results are in the range from 0.9 to 1.9 TPa,<sup>1,2</sup> *ab initio* results are in the range from 0.5 to 1.47 TPa,<sup>4-6</sup> empirical results are in the range from 0.971 to 0.975 TPa (Ref. 8) and from 1.11 to 1.258 TPa,<sup>9</sup> and also MD simulation results are in the range from 0.311 to 1.48 TPa.<sup>13-28</sup> Our calculated value at 300 K of 0.401 TPa is consistent with Refs. 4, 18, and 23. We determined the tensile strength of (10,10) tube as 83.23 GPa at 300 K and it decreases with increasing temperature. Maximum stress value of (10,10) tube is reported as 88 GPa in Ref. 10, and 77–101 GPa in Ref. 11. At 300 K, we calculated the Poisson ratio of (10,10) tube as 0.3. This is in accord with the *ab initio*,<sup>5</sup> empirical,<sup>8,11</sup> and tight-binding<sup>18</sup> results. Nardelli *et al.*<sup>24</sup> showed that all tubes are brittle at high strains and low temperatures, while at low strains and high temperatures armchair nanotubes can be completely or partially ductile. Our findings agree that this (10,10) armchair SWCNT is brittle at low temperatures and ductile at higher temperatures. Contrary to Ref. 28, our extensive temperature study has shown that Young's modulus changes with temperature.

## V. COMMENTS

Carbon nanotubes have the highest tensile strength of any material yet measured, with laboratories producing them at a tensile strength of 63 GPa, still well below their theoretical limit of 300 GPa. Carbon nanotubes are one of the strongest and stiffest materials known, in terms of their tensile stress and Young's modulus. This strength results from the covalent  $sp^2$  bonds formed between the individual carbon atoms. Our simulation study using the interactions between electrons and ions also predicts a similar tensile strength and also shows that when exposed to heat they still keep their tensile strength around this value until very high temperatures such as 1800 K. CNTs are not nearly as strong under compression. Because of their hollow structure and high aspect ratio, they tend to undergo buckling when placed under compressive stress. The elastic limit is the maximum stress a material can undergo at which all strains are recoverable (i.e., the material will return to its original size after removal of the stress). At stress levels below the elastic limit, the material is said to be elastic. Once the material exceeds this limit, it is said to have undergone plastic deformation (also known as

permanent deformation). When the stress is removed, some permanent strain will remain, and the material will be of a different size. Our study shows that when the nanotube is exposed to heat, this property does not change appreciably until 1800 K. Through our tight-binding molecular-dynamics simulation study, we reported the high-temperature positive and/or negative bond—breaking strain values and stress-strain curves of (10,10) SWCNTs. As far as we are aware, the strain energy values corresponding to positive and/or negative strain values at different temperatures hasn't been considered before. We hope that this extensive study of high-temperature mechanical properties will be useful for aerospace applications of CNTs.

## ACKNOWLEDGMENTS

The research reported here is supported through the Yildiz Technical University Research Fund Project No. 24-01-01-04. The calculations are performed at the Carbon Nanotubes Simulation Laboratory at the Department of Physics, Yildiz Technical University, Istanbul, Turkey.

\*Corresponding author. Electronic address: gdereli@yildiz.edu.tr

<sup>1</sup>A. Krishnan, E. Dujardin, T. W. Ebbesen, P. N. Yianilos, and M. M. J. Treacy, *Phys. Rev. B* **58**, 14013 (1998).

<sup>2</sup>M. F. Yu, B. S. Files, S. Arepalli, and R. S. Ruoff, *Phys. Rev. Lett.* **84**, 5552 (2000).

<sup>3</sup>D. Bozovic, M. Bockrath, J. H. Hafner, C. M. Leiber, H. Park, and M. Tinkham, *Phys. Rev. B* **67**, 033407 (2003).

<sup>4</sup>D. Sanchez-Portal, E. Artacho, J. M. Soler, A. Rubio, and P. Ordejon, *Phys. Rev. B* **59**, 12678 (1999).

<sup>5</sup>G. Zhou, W. Duan, and B. Gu, *Chem. Phys. Lett.* **333**, 344 (2001).

<sup>6</sup>A. Pullen, G. L. Zhao, D. Bagayoko, and L. Yang, *Phys. Rev. B* **71**, 205410 (2005).

<sup>7</sup>T. Dumitrica, T. Belytschko, and B. I. Yakobson, *J. Chem. Phys.* **118**, 9485 (2003).

<sup>8</sup>J. P. Lu, *Phys. Rev. Lett.* **79**, 1297 (1997).

<sup>9</sup>S. Gupta, K. Dharamvir, and V. K. Jindal, *Phys. Rev. B* **72**, 165428 (2005).

<sup>10</sup>T. Natsuki and M. Endo, *Carbon* **42**, 2147 (2004).

<sup>11</sup>X. Sun and W. Zhao, *Mater. Sci. Eng., A* **390**, 366 (2005).

<sup>12</sup>J. R. Xiao, B. A. Gama, and J. W. Gillespie, Jr., *Int. J. Solids Struct.* **42**, 3075 (2005).

<sup>13</sup>T. Ozaki, Y. Iwasa, and T. Mitani, *Phys. Rev. Lett.* **84**, 1712 (2000).

<sup>14</sup>B. Ni, S. B. Sinnott, P. T. Mikulski, and J. A. Harrison, *Phys. Rev. Lett.* **88**, 205505 (2002).

<sup>15</sup>L. G. Zhou and S. Q. Shi, *Comput. Mater. Sci.* **23**, 166 (2002).

<sup>16</sup>G. Dereli and C. Özdoğan, *Phys. Rev. B* **67**, 035416 (2003).

<sup>17</sup>S. Ogata and Y. Shibutani, *Phys. Rev. B* **68**, 165409 (2003).

<sup>18</sup>C. Goze, L. Vaccarini, L. Henrard, P. Bernier, E. Hernandez, and A. Rubio, *Synth. Met.* **103**, 2500 (1999).

<sup>19</sup>T. Xiao and K. Liao, *Phys. Rev. B* **66**, 153407 (2002).

<sup>20</sup>T. Xiao and X. Xu, *J. Appl. Phys.* **95**, 8145 (2004).

<sup>21</sup>M. Sammalkorpi, A. Krashennnikov, A. Kuronen, K. Nordlund, and K. Kaski, *Phys. Rev. B* **71**, 169906(E) (2005).

<sup>22</sup>Y. Wang, X. Wang, X. Ni, and H. Wu, *Comput. Mater. Sci.* **32**, 141 (2005).

<sup>23</sup>S. H. Yeak, T. Y. Ng, and K. M. Liew, *Phys. Rev. B* **72**, 165401 (2005).

<sup>24</sup>M. B. Nardelli, B. I. Yakobson, and J. Bernholc, *Phys. Rev. Lett.* **81**, 4656 (1998).

<sup>25</sup>N. R. Raravikar, P. Keblinski, A. M. Rao, M. S. Dresselhaus, L. S. Schadler, and P. M. Ajayan, *Phys. Rev. B* **66**, 235424 (2002).

<sup>26</sup>C. Wei, K. Cho, and D. Srivastava, *Phys. Rev. B* **67**, 115407 (2003).

<sup>27</sup>C. Wei, K. Cho, and D. Srivastava, *Appl. Phys. Lett.* **82**, 2512 (2003).

<sup>28</sup>Y. R. Jeng, P. C. Tsai, and T. H. Fang, *J. Phys. Chem. Solids* **65**, 1849 (2004).

<sup>29</sup>C. Özdoğan, G. Dereli, and T. Çağın, *Comput. Phys. Commun.* **148**, 188 (2002).

<sup>30</sup>G. Dereli and C. Özdoğan, *Phys. Rev. B* **67**, 035415 (2003).

<sup>31</sup>L. Colombo, *Comput. Phys. Commun.* **12**, 278 (1998).

<sup>32</sup>C. H. Xu, C. Z. Wang, C. T. Chan, and K. M. Ho, *J. Phys.: Condens. Matter* **4**, 6047 (1992).